

Procedure of the Multiple Indentations for Determination of the Hardness Parameters of Structurally Heterogeneous Materials

V. I. Kushch^{a,*}, S. N. Dub^a, R. S. Shmegeera^a, Yu. V. Sirota^a, and G. N. Tolmacheva^b

^a*Bakul Institute for Superhard Materials,
National Academy of Sciences of Ukraine,
vul. Avtozavods'ka 2, Kiev, 04074 Ukraine*

^b*Kharkiv Institute of Physics and Technology,
vul. Akademichna, 2, Kharkiv, 61108 Ukraine*

*e-mail: vkushch@bigmir.net

Received September 15, 2014

Abstract—A procedure of multiple indentations has been proposed as a promising method of studying surface properties of structurally heterogeneous bodies. It has been shown that this procedure is applicable to a wide spectrum of multiphase (including superhard) materials, ceramics, and metals and makes it possible to assess mean properties of separate phases and a composite as a whole as well as a degree of the sample hardness inhomogeneity at various scale levels. Such information is important in prediction of the wear and machinability of structurally heterogeneous materials. Experimental and model results that verify the efficiency of the procedure have been presented.

DOI: 10.3103/S1063457615030041

Keywords: hardness, indentation, structurally heterogeneous material, model, statistical analysis.

1. INTRODUCTION

At present methods of the indentation at the macrolevel are known [1–3]. These methods are directed to the microhardness measurement of homogeneous plastic materials, mainly metals and alloys. In the mechanics of rocks because of their inhomogeneity and brittleness, the concept of the aggregate (averaged) hardness is used. The common feature of these methods is that the size of the indenter imprint is much larger than the characteristic length of the material structural inhomogeneity. The method of the microhardness determination [4] is designed to assess the hardness of small (microscopic) volumes of materials, in particular separate phases or structural components of the alloys. In measurements of microhardness a Vickers indenter is most often used in the loading range from 0.05 to 5 N. The nanoindentation method [5–7], which is intensively progresses in recent years, is directed at the studies of mechanical properties of nanovolumes of materials and thin films under very low loads. The method is based on the analysis of the indenter load–displacement curve, which is used for determining hardness and elastic modulus of the material. Nanoindenters, as a rule, are equipped by a Berkovich indenter and the depth of its imprints ranges from units to hundreds of nanometers.

Despite the difference between the length scales of the above procedures, all of them imply the uniformity of the material under study. This assumption is in the evident contrast with the fact that the absolute majority of the real materials are structurally heterogeneous and often are characterized by the essential volumetric inhomogeneity of properties. This leads to a considerable scatter of the hardness values of such materials obtained by indentation. Therefore, to study structurally heterogeneous materials, it seems advisable to use the proposed procedure of multiple indentations with a subsequent statistical processing of the measurements results. This approach is promising at least in two directions. Firstly, the statistical analysis allows us to essentially reduce the instrumental error and evaluate the real accuracy of the data obtained. Secondly, which even is more important, it offers considerable additional information about the material under study, in particular the assessment of the degree of the sample hardness inhomogeneity and its statistical characteristics in studying at different length scales. Such information is important for prediction of wear and machinability of structurally heterogeneous materials (e.g., [8–10]).

2. SCALE FACTOR IN INDENTATION OF STRUCTURALLY INHOMOGENEOUS MATERIALS

In studying structurally heterogeneous materials by indentation we deal at least with two dimensional quantities. One of them is the size of an imprint; the other is a characteristic length of the structure inhomogeneity.

generality. As a consequence, the indentation results depend considerably on the relation between the above sizes, i.e., the scale factor takes place.

For simplicity we consider a material consisting of two phases with different mechanical properties and characteristic lengths of inhomogeneities, d (Fig. 1). The size of the Vickers indenter imprint is defined by the depth, h , or the length of the square side $l = 5h$. If the imprint depth is much less than the characteristic length of the phase ($h \ll d$), the test result is defined by the properties of one of the phases. As a great number of tests are performed, the probability to meet one or the other phase is equal to a specific area occupied by this phase on the surface under study. If the maximum depth of the imprint is much greater than the characteristic length of the inhomogeneities ($h \gg d$), from such an experiment the average (in the statistical sense) properties of the structurally heterogeneous material are defined.

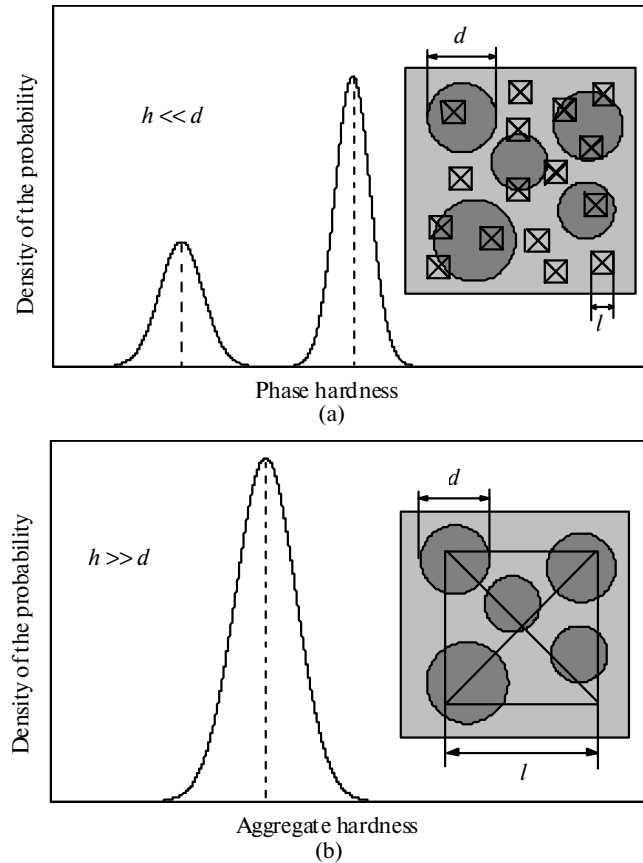


Fig. 1. Scheme of the indentation of structurally heterogeneous materials: low (a) and great (b) depths of indentations.

In addition to the characteristic length of inhomogeneities (e.g., size of inclusions), which is denoted as d , it is necessary to introduce into consideration a characteristic length, d_s , of the material volume deformed during the indentation of the multiphase material. The indentation result depends mainly on the material properties in the neighborhood of the indenter tip, therefore, as the d_s one may use the diameter of a half-sphere under the indenter, which is defined by isolines of the resultant stress field. At $d_s < d$ the indentation is restricted to one phase and characterizes its properties. The deformed volume depends on the indentation depth, h , indenter geometry, and properties of the studied material (Young modulus, E ; Poisson's ratio, ν ; hardness, H ; angle of internal friction, α ; and characteristic size of inhomogeneity, d). The dimensional analysis of the problem is given in [11]:

$$\frac{d_s}{h} = \Pi_{d_s} \left(\theta, \frac{E}{H}, \nu, \alpha, \frac{h}{d} \right). \quad (1)$$

The first four invariants are properties of the structurally heterogeneous material, while h/d binds the imprint size with the characteristic length of inhomogeneity. If the h/d tends to zero, h is the only measure of length in an infinite half-space and the problem meets the condition of the self-similarity. The properties (E , H) found by the indentation at $h \ll d$ are characteristics of the phase of size d , while the indentation at $h \gg d$ defines the properties of a composite.

Thus, the classic method of tool indentation may be expanded to include the class of heterogeneous materials on condition that the indentation depth, which depends on the characteristic length of inhomogeneity, is the properly chosen. This requires a series of tests with a subsequent statistic analysis of the data obtained. The choice of the critical depth of the indentation, h_{crit} , at which the phase properties are still possible to measure reliably by indentation, is justified by both analytical and numerical studies. Thus, the aim of the numerical modeling in [12] was to measure hardness by a cone indenter of almost ideally plastic two-phase system. As is shown by the calculations, for a contact radius $< 0.7 d$ the hardness of a separate phase is measured correctly, and h_{crit} depends weakly on the form of the indented phase and is defined first of all by its characteristic length d .

3. STATISTICS OF MULTIPLE INDENTATIONS

The presence of the scale factor in studying structurally heterogeneous materials by indentation complicates the procedure of the analyzing results. The first problem in this case is the choice of the distribution function for each peak of empirical or frequency density, which is unambiguously defined by its statistic moments. If the measurements and the material itself were ideal, for small imprints one should expect the distribution density in the form of separate peaks that are characterized by the first instant only (the mean value). However, there is a number of reasons resulted in the blurring of the histogram peaks. Firstly, the measurement themselves introduce an accidental error; secondly, the properties of each phase have its own internal changeability; thirdly, the indenter imprints are not infinitely small. Therefore, the analysis of experimental data requires that the statistical moments of higher order should be considered.

The designations of statistical parameters used from here on correspond to [13]. The integral function of distribution of the continuous random quantity, ξ , is

$$F_{\xi}(x) = \Pr(\xi \leq x) = \int_{-\infty}^x p_{\xi}(t) dt, \tag{2}$$

where $p_{\xi}(t) = \frac{d}{dx} F_{\xi}(x)$ is the density of probability. The mean value (mathematical expectation) of E , dispersion, D , and root-mean-square (standard) deviation, SD , of the random quantity, ξ , are defined by the relations

$$E[\xi] = \int_{-\infty}^{\infty} t dF_{\xi}(t); D[\xi] = (SD[\xi])^2 = \int_{-\infty}^{\infty} (t - E[\xi])^2 dF_{\xi}(t). \tag{3}$$

The corresponding empirical parameters for a finite set, N , of realizations of the random quantity (in our case, the ordered sample of the measurements results) $\xi = \{\xi_n\}_{n=1}^N$ look like

$$\hat{E}[\xi] = \frac{1}{N} \sum_{n=1}^N \xi_n; \hat{D}[\xi] = \frac{1}{N-1} \sum_{n=1}^N (\xi_n - \hat{E}[\xi])^2. \tag{4}$$

Empirical function of distribution for a finite sample is

$$\hat{F}_{\xi}(x) = \Pr(\xi_n \leq x) = \sum_{\xi_n \leq x} p_n, \tag{5}$$

where p_n is the probability $\Pr(\xi = \xi_n)$ in this experiment.

As it was established in [14], for a statistical description of mechanical properties of each phase the normal distribution, which is determined by the mean value $E[\xi] = \mu_{\xi}^j$ and $SD[\xi] = s_{\xi}^j$ standard deviation, is:

$$p_{\xi}(x) = \frac{1}{\sqrt{2\pi}s_{\xi}} \exp\left[-\frac{(x - \mu_{\xi})^2}{2s_{\xi}^2}\right]. \tag{6}$$

To identify its parameters, the empirical function of distribution $\hat{F}_{\xi}(x)$ (Eq. (5)) is used. In our case

$$\hat{F}_{\xi}(\xi_i) = \frac{1}{N} \left(i - \frac{1}{2}\right), i = 1, 2, \dots, N. \tag{7}$$

In the general case it is presumed that a structurally heterogeneous material consists of n phases with the sufficient contrast of mechanical properties and the volumetric/surface content of the phase j is c_j . The mean value $E[\xi] = \mu_\xi^j$ and standard deviation $D[\xi] = s_\xi^j$ for each phase is defined by minimization of the function [14]

$$\sum_{i=1}^N \left(\sum_{j=1}^n c_j \Phi(\xi_i; \mu_\xi^j, s_\xi^j) - \hat{F}_\xi(\xi_i) \right)^2. \quad (8)$$

The condition for the volumetric fractions of various phases is evidently $\sum_{j=1}^n c_j = 1$.

4. VERIFICATION OF THE PROCEDURE: VIRTUAL EXPERIMENT

The proposed procedure is applicable for studying heterogeneous structures of the general type. To verify the efficiency and demonstrate potentialities of the procedure, we shall make the following computer experiment on two-phase composite material that consists of one continuous phase (a matrix) and randomly located discrete inclusions of the second phase. For decreasing the number of parameters, inclusions are assumed to be round and equal in size (with diameter d). The location of the Vickers indenter imprint within the structure cell in multiple indentations is defined either by a sensor of random numbers or by points of the uniform grid. The latter may be realized in the experiment with the use of a nanoindenter with a programmable behavior. We considered three sizes of imprint l (see Fig. 1): $l = 0.1d$ (small imprint), $l = d$ (mean imprint), and $l = 3d$ (large imprint).

Following the authors of [14], we assume that hardness of the matrix phase materials, H_1 , and of inclusions, H_2 , are distributed according to the normal law (6) with parameters μ^1, s^1 and μ^2, s^2 , respectively. In the case that the part f_1 of the imprint area $S_1 = f_1 l^2$ is occupied by the matrix phase and $S_2 = f_2 l^2$ ($f_1 + f_2 = 1$, $S = S_1 + S_2$) by inclusions, the measured hardness is taken to be proportional to partial fractions of the phases: $H = f_1 H_1 + f_2 H_2$. For the practical calculations we assume that $\mu^1 = 3.5$ GPa, $\mu^2 = 9.25$ GPa and $s^1 = s^2 = 0.7$ GPa.

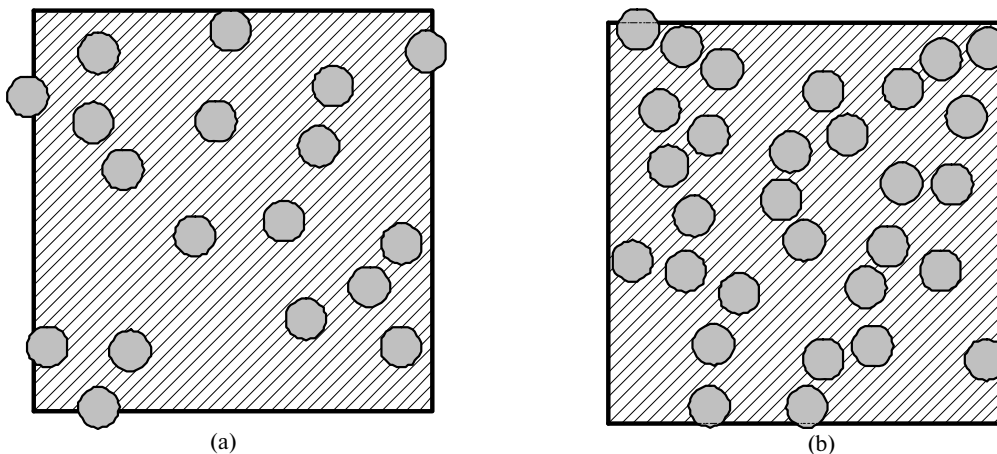


Fig. 2. Representative cell of the structure of a model two-phase material with different contents of the dispersed phase $c_2 = 1 - c_1$: $c_2 = 0.15$ (a), 0.3 (b).

Figures 3–5 show the calculated histograms of the densities of hardness distributions of two-phase composites at the given parameters and the results of the histograms approximations by function (8). To ensure statistical importance of calculated data, for each set of parameters a random sampling of hardness consisted of 10^4 values and the range of changes was divided into 50 intervals of the same length. Since the geometric model is constructed with the use of a probabilistic approach, the method to choose the indentation points is of no importance. The experience in calculations shows that a periodical (quadratic) and disordered sets of imprints give virtually coinciding hardness values.

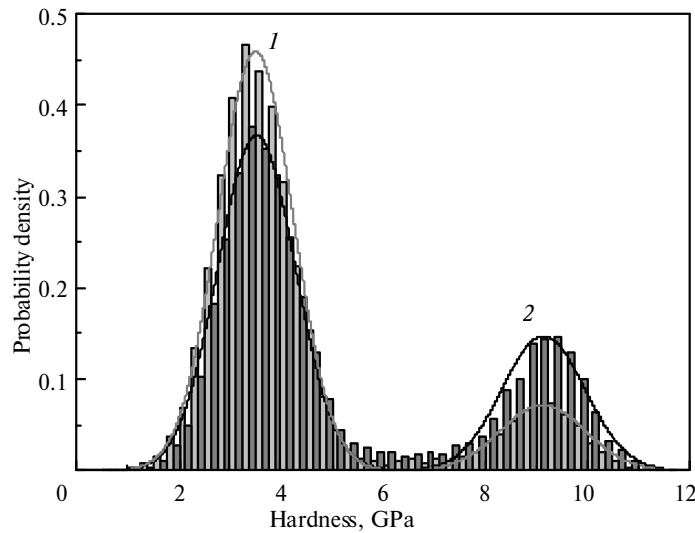


Fig. 3. Calculated histogram of the hardness distribution density in a model composite with $c_2 = 0.15$ (1) and $c_2 = 0.3$ (2); the imprint size $l = 0.1d$; the solid curve is the approximation by Eq. (8).

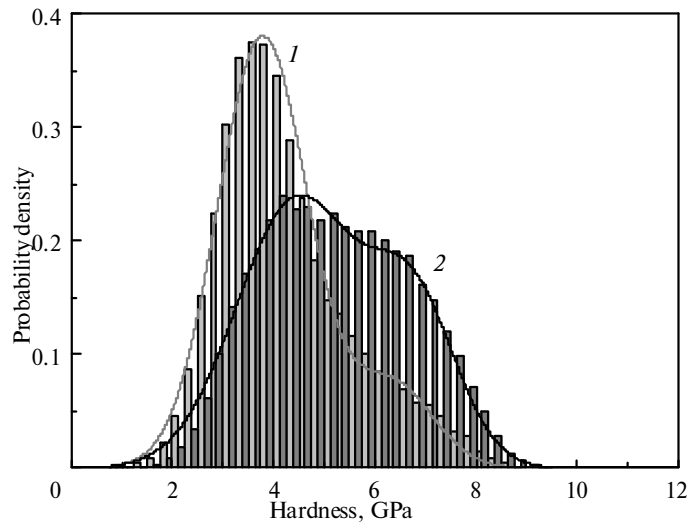


Fig. 4. Calculated histogram of the hardness distribution density in a model composite with $c_2 = 0.15$ (1) and $c_2 = 0.3$ (2); the imprint size $l = d$; the solid curve is the approximation by Eq. (8).

As is seen from the figures, function (8) offers a satisfactory approximation of the results of computer modeling over the whole range of l/d relations. The values of μ^1, s^1 and μ^2, s^2 parameters obtained by solving an optimization task are given in Table 1.

Table 1. Results of the approximation of empirical histograms by function (8)

	$l = 0.1d$		$l = d$		$l = 4d$	
c_2	0.15	0.30	0.15	0.30	0.15	0.30
μ^1, GPa	3.50	3.52	3.79	4.46	4.31	5.31
s^1, GPa	0.74	0.76	0.89	1.18	0.64	0.59
μ^2, GPa	9.14	9.15	6.34	6.76	3.64	4.65
s^2, GPa	0.83	0.81	0.80	0.85	0.61	0.61
E, GPa	4.35	5.22	4.29	5.21	4.21	5.11
SD, GPa	2.10	2.61	1.32	1.47	0.67	0.67

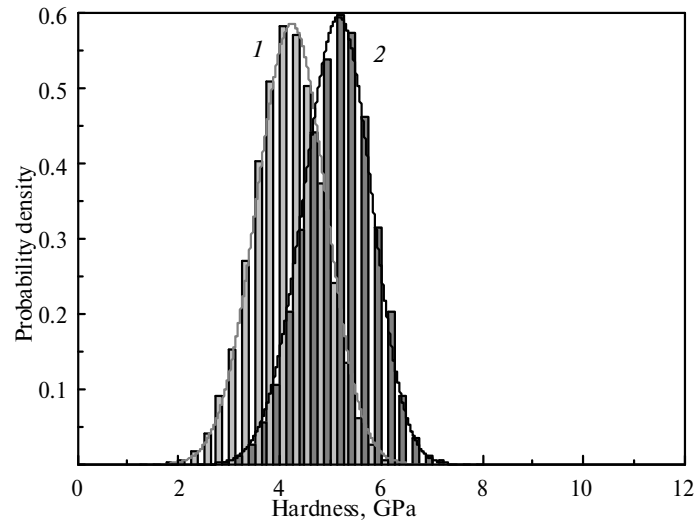


Fig. 5. Calculated histogram of the hardness distribution density in a model composite with $c_2 = 0.15$ (1) and $c_2 = 0.3$ (2); the imprint size $l = 4d$; the solid curve is the approximation by Eq. (8).

It follows from the table that in the case of small (compared with inclusions) imprints the recovered values of statistical parameters are close to the initial. This gives ground to speak about the correctness of the procedure and reliability of the modeling results. More important conclusion is that the procedure affords adequate determination of statistical parameters of hardness of separate phases with the proviso that $h \ll d$. For the case of $h \gg d$ the modeling predicts an approachment of statistical parameters. It follows from Figs. 3–5 and Table 1 that as the load/imprint increases, the statistical distribution of hardness approaches to the standard distribution with mean values of 4.2 GPa for $c_2 = 0.5$ and 5.1 GPa for $c_2 = 0.3$. It should be noted that the above mean hardness values practically coincide with empirical mean E calculated from the results of modeling (the last but one line of Table 1). In this case the size effect is low. On the contrary, the standard deviation SD (the last line of Table 1) increases quite expectedly as the imprint size decreases and therefore, may be used as an indirect characteristic of the degree of the material structure inhomogeneity.

5. VERIFICATION OF THE PROCEDURE: FULL-SCALE EXPERIMENT

The proposed procedure was tested on the two-phase material produced by intensive electric sintering of nickel and tin powders [15, 16]. By analogy with the model experiment, two samples were taken with 6 and 12 wt % of tin; from here on they will be denoted Ni–6Sn and Ni–12Sn, respectively. The intensive electrical sintering of samples was carried out by direct passing the power current through the sample and simultaneously applying a pressure of 150 MPa to it. The examination of the sintered sample by scanning electron microscopy in [16] showed that its structure was virtually free from pores, macroscopically uniform and consisted of two phases: nickel and intermetallic Ni_3Sn . The volumetric content of the intermetallic of the sintered material exceeds the tin content of the initial mixture by a factor of 2.5, therefore, here as in the model experiment, $c_2 = 0.15$ for Ni–6Sn and $c_2 = 0.3$ for Ni–12Sn. What is important for this study, the material has the developed microstructure with a characteristic length, d , of about 10 μm (Fig. 6) and has a considerable contrast of phases properties.

The tests at low loading (5 mN) were conducted on a Nano Indenter G200 device (Agilent Technologies, USA). Each sample was subjected to 200 runs and the imprints were located in a square order at a distant of 20 μm from one another (see Fig. 6). The light regions in a photo correspond to nickel and dark to Ni_3Sn intermetallic. It is seen even with an unaided eye that imprint 2 in nickel is considerably larger and therefore, hardness is lower than in intermetallic phase (imprint 1). The indenter load-displacement curves corresponding to these imprints are given in Fig. 7 and it follows from the figure that the maximum depth of the indenter penetration into nickel at a load of 5 mN is 220 nm, while the penetration into Ni_3Sn is 130 nm only. The hardness is known to be proportional to the square of the imprint linear size and, hence, the hardness values differ approximately by a factor of 3.

Histograms constructed from the tests results (empirical probability densities) for Ni–6Sn and Ni–12Sn materials are shown in Figs. 8 and 9, respectively. The approximations of empirical histograms by function (8) are indicated by solid lines in the figures and identified distribution parameters are given in the first two col-

umns of Table 2. These data are close to those given in Fig. 3 and Table 1. This is quite expectable result, as the imprint size, l , is about $1\ \mu\text{m}$, i.e., the condition $l \approx 0.1d$ is fulfilled. The closeness of the predicted by the model and measured values is predetermined by the proper choice of the input parameters for a virtual experiment, see section 4. It is noteworthy that empirical mean values calculated by Eq. (4) are 4.3 and 5.0 GPa for Ni–6Sn and Ni–12Sn, respectively, i.e., they practically coincide with those obtained in a virtual computer experiment.

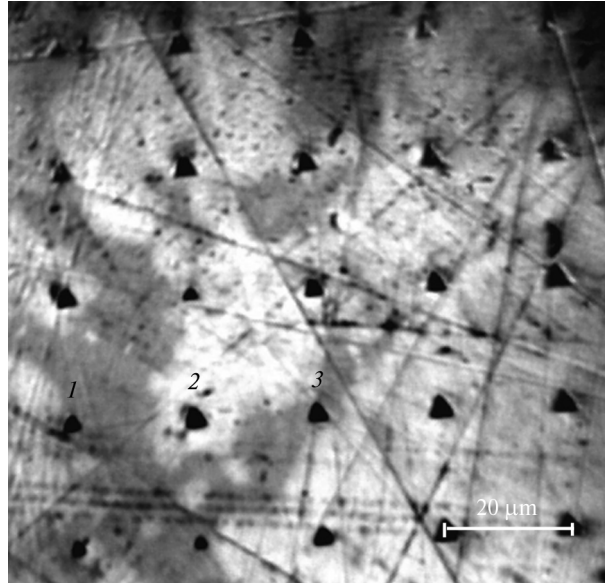


Fig. 6. Fragment of the Ni–6Sn structure with a square net of imprints in intermetallic (1), nickel (2), and in a mixture of phases (3); the spacing between imprints is $20\ \mu\text{m}$.

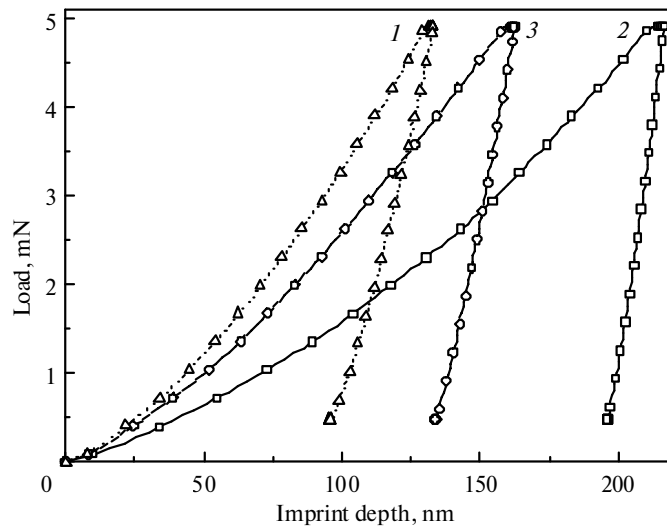


Fig. 7. Nanoindenter load–displacement curves in intermetallic (1), nickel (2), and mixed (3) phases of the Ni–6Sn material.

Table 2 gives also the results of the similar statistical analysis of the data on microhardness ($P = 0.2\ \text{N}$) and macrohardness ($P = 2.0\ \text{N}$) of Ni–6Sn and Ni–12Sn obtained using a PMT-3 hardness tester. These results differ essentially from those observed in the computer experiment where empirical mean values were insensitive to the load value. Therefore, a decrease in the mean hardness as the load increases is unambiguously due to a size effect of the hardness. At low loads the hardness strongly depends on the imprint depth: according to [17], the Vickers hardness of nickel of grade Ni 200 is $H_V = 1.7\ \text{GPa}$ for $h > 20\ \mu\text{m}$, $H_V = 2.2\ \text{GPa}$ for $h = 10\ \mu\text{m}$, and $H_V = 3.7\ \text{GPa}$ for $h = 1\ \mu\text{m}$. The last value is close to μ^1 , obtained by a statistical analysis of the data file for two different materials, which allows us to speak both of the reliability of these data and adaptability of the procedure for assessing hardness of individual phases of a structurally heterogeneous material. As

far as we know, there is no information in the literature of mechanical properties of the Ni₃S intermetallic. This procedure predicts its hardness within 8.4–9.2 GPa. We were the first to obtain these values as well as the indenter load–displacement dependence for Ni₃Sn (see Fig. 7, curve 3).

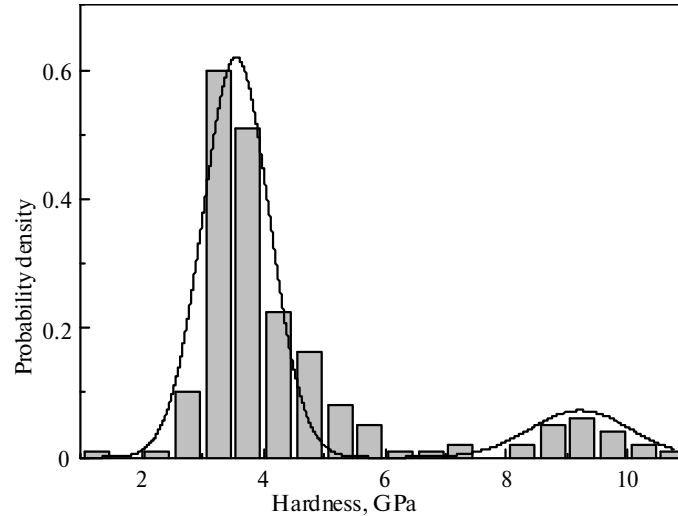


Fig. 8. Histogram of Ni–6Sn hardness ($c_2 = 0.15$, $P = 5$ mN), the solid curve is the approximation by Eq. (8).

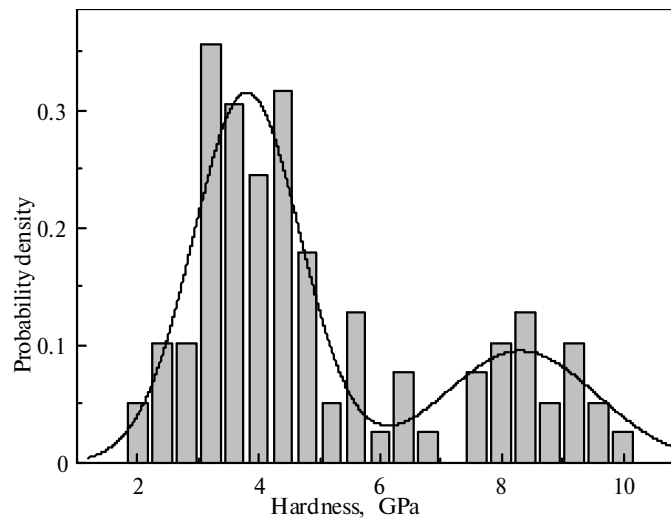


Fig. 9. Histogram of Ni–12Sn hardness ($c_2 = 0.3$, $P = 5$ mN), the solid curve is the approximation by Eq. (8).

Table 2. Results of the approximation of empirical histograms by function (8)

Device	Nano Indenter G200 Berkovich indenter $P = 5$ mN		PMT-3 Vickers indenter $P = 0.2$ N		PMT-3 Vickers indenter $P = 2.0$ N	
	Ni–6Sn	Ni–12Sn	Ni–6Sn	Ni–12Sn	Ni–6Sn	Ni–12Sn
Sample						
μ^1 , GPa	3.55	3.83	2.08	2.02	1.39	1.44
s^1 , GPa	0.54	0.90	0.67	0.34	0.43	0.26
μ^2 , GPa	9.21	8.34	3.95	3.69	2.38	2.35
s^2 , GPa	0.82	1.22	0.49	0.23	0.18	0.11
E , GPa	4.33	5.0	2.50	2.43	1.62	1.63
SD , GPa	1.79	2.13	1.26	0.75	0.58	0.27

5. CONCLUSIONS

The procedure of the multiple indentations has been found to be a promising method for studying surface properties of the phases of structurally heterogeneous materials. It has been established that the procedure is applicable to a wide sphere of multiphase (in particular, superhard) materials, ceramics, and metals and allows one to evaluate the mean properties of separate phases of a composite and volume content of them.

The experimental and model results in the hardness of composite materials, which have been obtained in our study, are indicative of the efficiency of the procedure and its sufficient resolution. The procedure is characterized by the fact that the hardness distribution at the level of components is normal, while at the macrolevel it changes depending on the indentation load. It has been predicted that in using the instrumental indentation technique with registration of the indentation diagram a similar approach may be extended to investigations of elastic and plastic properties of structurally heterogeneous materials.

Function (8) affords a sufficient approximation of the results obtained by the hardness measurements over the whole range of the relations between the imprint size and characteristic length of the inhomogeneity. The additional data on the material under study that have been obtained include the assessment of the degree of the hardness inhomogeneity over the sample and its statistical characteristics at different lengths may be used for a more precise prediction of the wear and machinability of structurally heterogeneous materials.

It is worthwhile to further develop the procedure by considering a type of the microstructure, method of determining the characteristic length of inhomogeneity, and introducing “physical” size effects that manifest themselves at low indentation loads into consideration.

REFERENCES

1. Tabor, D., *Hardness of Metals*, Oxford: Oxford University Press, 1951.
2. Johnson, K.L., *Contact mechanics*, Cambridge: Cambridge University Press, 1985.
3. Bulychev, S.I. and Alekhin, V.P., *Ispytanie materialov nepreryvnyim vdavlivaniem indentera* (Testing materials by continuous indentation), Moscow: Mashinostroenie, 1990.
4. GOST 9450-76, Measurement of microhardness by penetration of diamond tips.
5. Oliver, W.C. and Pharr, G.M., An improved technique for determining hardness and elastic modulus using load and displacement sensing indentation experiments, *J. Mater. Res.*, 1992, vol. 7, no. 6, pp. 1564–1583.
6. Fischer-Cripps, A.S., *Nanoindentation*, New York: Springer, 2004.
7. Kushch, V.I. and Dub, S.N., The assessment of elastoplastic properties of materials from nanoindentation and computer modeling. 1. State-of-the-art of the problem (Review of the literature), *J. Superhard Mater.*, 2012, vol. 34, no. 3, pp. 149–155.
8. Fedorchenko, I.M., Modern theories of the mechanism of friction and wear and the main trends in the development of composite frictional and bearing materials. A review, *Poroshkovaya Metallurgiya*, 1979, no. 4, pp. 53–65.
9. Zhang, Z., Zhang, L., and Mai, Y.-W., Modelling friction and wear of scratching ceramic particle reinforced metal composites, *Wear*, 1994, vol. 176, pp. 231–237.
10. *Sverkhtverdye materialy. Poluchenie i primenenie* (Superhard materials. Production and application), 6 vols, Novikov, N.V., Ed., *Obrabotka materialov lezviinym instrumentom* (Machining Materials with Cutting Tools), vol. 5, Klimenko, S.A., Ed., Kiev: Bakul' ISM, National Academy of Sciences of Ukraine, 2006.
11. Randall, N.X., Christoph, R., Droz, S., and Julia-Schmutz, C., Localized microhardness measurements with a combined scanning force microscope/nanoindentation system, *Thin Solid Films*, 1996, vol. 291, pp. 348–354.
12. Durst, K., Goken, M., and Vehoff, H., Finite element study for nanoindentation measurements on two-phase materials, *J. Mater. Res.*, 2004, vol. 19, pp. 85–93.
13. Cramer, H., *Mathematical methods of statistics*, Uppsala: Almqvist and Wiksells, 1945.
14. Randall, N.X., Nanoindentation analysis as a two-dimensional tool for mapping the mechanical properties of complex surfaces, *J. Mater. Res.*, 2009, vol. 24, pp. 679–690.
15. Shmegera, R.S., Intensive electric sintering of metal matrices of diamond-containing composites in the presence of a liquid phase, *Porodorazrushayushchii i metallobrabatyvayushchii instrument—tehnika i tekhnologiya ego izgotovleniya i primeniya* (Rock Destruction and Metal-Working Tools—Techniques and Technology of the Tool Production and Applications), Collect. Sci. Papers, Kiev: Bakul' ISM, Nat. Acad. Sci., 2012, issue 15, pp. 507–510.
16. Shmegera, R.S., Kushch, V.I., and Maistrenko, A.L., Metal binder based on nickel for an intensive electrosintering of diamond-containing composites, *J. Superhard Mater.*, 2014, vol. 36, no. 6, pp. 393–400.
17. Yovanovich, M.M., Micro and macro hardness measurements, correlations, and contact models, Proc. 44th AIAA Aerospace Sciences Meeting and Exhibit, 9–12 January 2006, Reno, Nevada, USA.

Translated by G. Kostenchuk